276 | https://doi.org/10.3311/PPci.16996
Creative Commons Attribution

Periodica Polytechnica Civil Engineering, 65(1), pp. 276–286, 2021

Performance Evaluation of Pre-foamed Ultra-lightweight Composites Incorporating Various Proportions of Slag

Trong-Phuoc Huynh[1*], Van-Hien Pham[1], Ngoc-Duy Do[2], Trong-Chuc Nguyen[3], Nguyen-Trong Ho[4]

[1] Department of Civil Engineering, College of Engineering Technology, Can Tho University, Campus II, 3/2 St., Ninh Kieu Dist., Can Tho City 900000, Vietnam
[2] Department of Civil and Construction Engineering, National Taiwan University of Science and Technology, No. 43, Sec. 4, Keelung Rd., Da'an District, Taipei City 10607, Taiwan
[3] Institute of Special Construction Engineering, Le Quy Don Technical University, Hanoi 100000, Vietnam
[4] Faculty of Civil Engineering, VSB-Technical University of Ostrava, Ludvika Podesta 1875/17, 708 00 Ostrava-Poruba, Czech Republic
[*] Corresponding author, e-mail: htphuoc@ctu.edu.vn

Received: 08 August 2020, Accepted: 11 October 2020, Published online: 09 November 2020

Abstract

This research examines the feasibility of using a mixture of cement, fly ash, ground granulated blast-furnace slag, and river sand to manufacture pre-foamed ultra-lightweight composite (PULC). Four PULC specimens were prepared with the substitution of cement by slag at 0, 10, 20, and 30 % by weight. The engineering properties of PULC samples were evaluated through the tests of compressive strength, dry density, water absorption, drying shrinkage, and thermal conductivity. Besides, numerical simulation of heat transfer through the PULC brick wall and the microstructure observation were performed. The performance of PULC mixtures incorporating slag showed higher effectiveness than merely used cement. The substitution of 20 % cement by slag resulted in the highest compressive strength as well as the lowest value of water absorption of the PULC samples. Also, the efficiency of the thermal conductivity was in inverse proportion with the density of PULC specimens and it was right for water absorption and drying shrinkage. Moreover, numerical simulations showed that the temperature distribution values in the wall made by PULC material were smaller than in the wall made by the normal clay brick in the same position. Besides, the microstructure analysis revealed that the existence of slag generated a more dense structure of PULC samples with the addition of calcium-silicate-hydrate (C-S-H) gel, especially for a mix containing 20 % slag. Thus, the results of this study further demonstrated that a 20 % slag was the optimal content for the good engineering properties of the PULC samples.

Keywords

pre-foamed ultra-lightweight composite, simulation of heat transfer, thermal conductivity, drying shrinkage, microstructure

1 Introduction

In recent years, people find out many alternative binders to substitute the ordinary Portland cement (OPC) in order to decrease the negative influence of cement manufacture and consumption in the construction industry. The harmful effects on the natural environment are always essential issues of OPC production that were referred by previous researches [1, 2]. Therefore, OPC manufacture is one of the principal factors inducing the overall emission of greenhouse gases (about 8–10 % [3]) in recent decades. On the other hand, to catch up on the speed of construction development, it is necessary to apply modern technologies into practices to not only enhance the project quality but also accelerate the construction progress. In fact, the precast structures created by composites material has been recently used in many developed countries due to the dominant features such as light, thermal and sound insulation, and time- and cost-saving. Notably, the foam concrete has been known as a kind of sustainable lightweight construction material with some advantages of the cost decrease, the optimization of insulation, and enhancing the fire resistance of structures [4]. Moreover, it also provides a quick and settlement-free building with good thermal insulation [5]. However, global warming due to the construction process, especially the cement production impulses the co-friendly substitute

Cite this article as: Huynh, T.-P., Pham, V.-H., Do, N.-D., Nguyen, T.-C., Ho, N.-T. "Performance Evaluation of Pre-foamed Ultra-lightweight Composites Incorporating Various Proportions of Slag", Periodica Polytechnica Civil Engineering, 65(1), pp. 276–286, 2021. https://doi.org/10.3311/PPci.16996

development for cement, and the research of new construction material applications is a priority. Consequently, the utilization of industrial by-products as binder materials in foam concrete compositions was a timely solution.

Fly ash (FA) and ground granulated blast furnace slag (so-called slag) have been used as viable materials in concrete, aiming to the development of eco-friendly and sustainable material [6, 7]. Similarly, there were several studies conducted to evaluate the effects of slag as cement replacement materials on the properties of foam concrete [8, 9]. Accordingly, the replacement of cement by ultrafine slag exhibited a marginal increase in the compressive strength of foam concrete [10]. Besides, the foam concrete had lower porosity and permeability values with the addition of slag [11]. Economically, the use of slag was beneficial in reducing the concrete cost and also redeeming the financial values from the steel manufactures [12]. Nevertheless, the utilization of slag in the production of pre-foamed ultra-lightweight composites (PULC) has not been referred to yet and reported in researches until now. Hence, this paper studied the performance of PULC samples incorporating slag as a partial replacement of cement in the PULC mixtures. PULC is a kind of foam concrete known as a flowable material with low compaction and vibration, but high requirements for production and curing conditions. Correspondingly, in order to provide the best insulation to heat and sound, the quality of foam is the most important factors so the pre-foamed technique is applied to control the performance of PULC. Besides, input materials are carefully prepared to guarantee special attributes of PULC, especially an ultra-lightweight material.

In this experimental study, the effects of various amounts of slag on the performance of PULC samples were investigated. Changes in engineering properties of PULC mixtures such as compressive strength, density, water absorption, drying shrinkage, and thermal conductivity were analyzed. In addition, scanning electron microscope (SEM) images and X-ray diffractometer (XRD) patterns of samples before and after reaction were also performed to understand the behaviors of slag and FA in the hydration of cement-based system. Besides, to save energy and increase the ability of insulation for the building, a numerical simulation of heat transfer through the wall modeled by conventional clay brick and the developed PULC material was also conducted in this research to exhibit the effectiveness of lowering environmental impacts.

2 Materials and mixture proportions

2.1 Material properties

The natural appearance of the raw materials used in this study is shown in Fig. 1. As shown in Fig. 1(a), local grade-40 cement with dark grey color was used for the laboratory

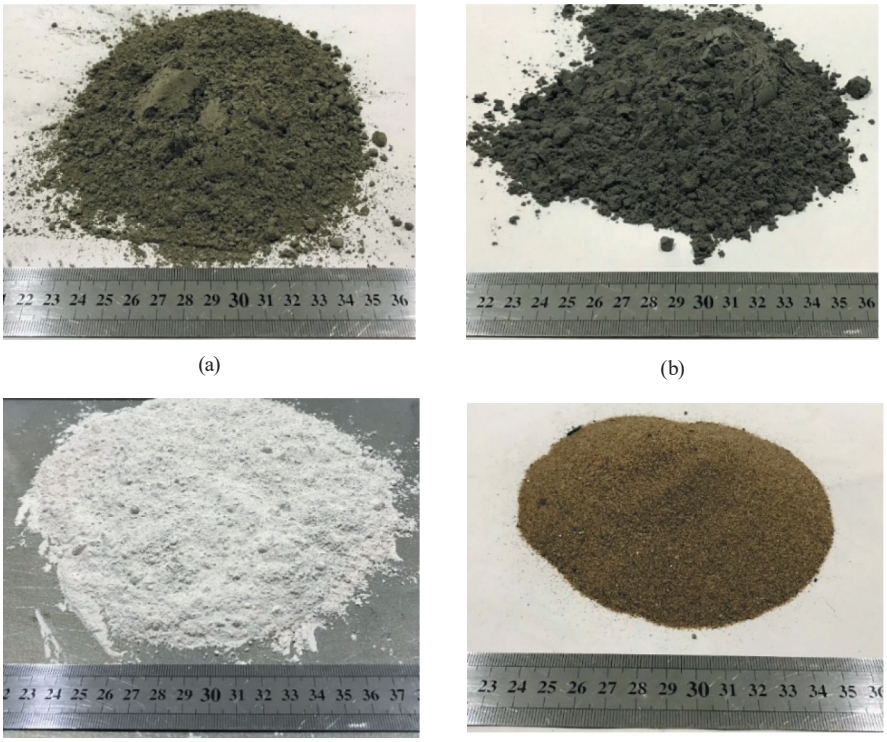

Fig. 1 The natural appearance of raw materials: a) cement, b) FA, c) Slag, d) sand

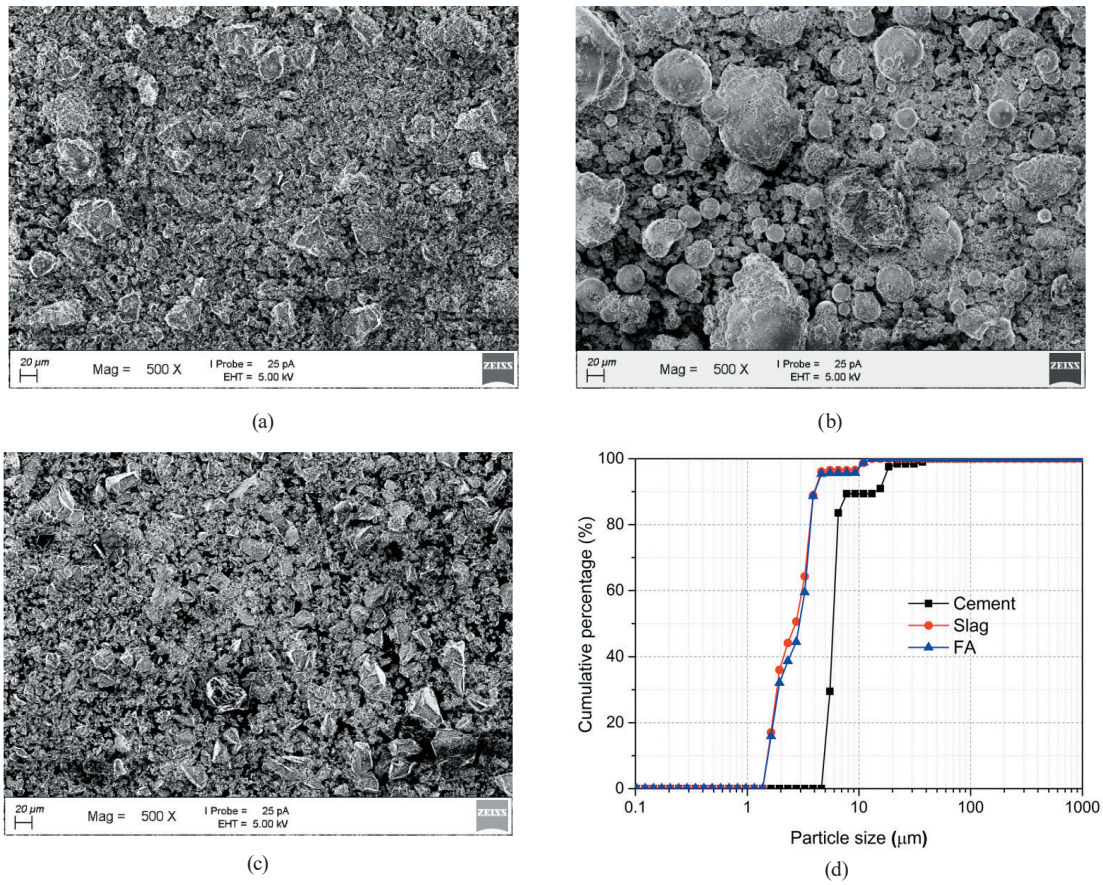

Fig. 2 SEM images and grain size distribution of raw materials: a) cement, b) FA, c) Slag, d) Grain size distribution

test throughout this investigation and the microscopic image (Fig. 2(a)) presented that cement particles are angular and irregular in shape. Grain size distribution and XRD pattern of cement were presented in Fig. 2(c) and Fig. 3, respectively. FA from a thermal power plant in Tra Vinh province of Viet Nam was used to partially substituted for cement and the natural appearance of FA is shown in Fig. 1(b) with a dark black color. Also, based on the chemical compositions of FA as given in Table 1, the classification of this FA was F-type based on the ASTM C618 standard [13].

As presented in Fig. 2(b), while round in shape FA particles made up a major composition, there were rough and un-smooth ones that distributed among FA particles. Besides, the gradation curve of FA was smaller than cement and quite similar to slag and it can be noticed that the utilization of FA enables the structure of PULC samples to modify the physical and chemical aspects. However, the XRD pattern of FA in Fig. 3 had more crystalline phases (narrow and intense peaks) of mullite and quartz and indicated a low degree of reactivity. In comparison with FA, slag particles had a white color (Fig. 1(c)), the shape of the particles was similar to cement (Fig. 2(c)), but the particles of slag were much smaller (Fig. 2(d)) and mostly in amorphous phase (Fig. 3). The amorphous phase of slag indicated its high degree of reactivity. The various proportions of oxides present in cement, FA, and slag were reported in Table 1. As compared with cement, slag had a smaller amount of CaO but higher contents of SiO_2 and Al_2O_3, indicating that the addition of slag could support for the secondary reaction owing to the reactions between SiO_2 and Al_2O_3 with the alkaline environment

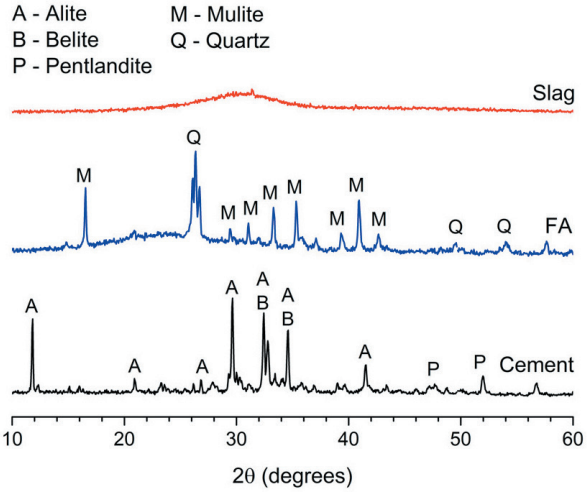

Fig. 3 XRD analysis of raw materials

Table 1 Chemical compositions of raw materials

CMs	SiO_2	Al_2O_3	Fe_2O_3	MgO	CaO	Others
Cement	23.49	6.01	3.65	1.98	59.89	4.98
FA	59.17	26.71	6.06	0.89	1.07	6.10
Slag	35.88	12.99	0.32	7.99	38.13	4.69

(created from the hydration reaction between CaO and water) to produce more calcium-silicate-hydrate (C-S-H) gels. Similarly, a higher proportion of SiO_2 and Al_2O_3 in FA (greater than slag) was very advantageous for the hardening processes of PULC samples.

River sand (Fig. 1(d)) with a density of 2.61 g/cm^3 and fineness modulus of 1.3 was used as fine aggregate of PULC mixtures.

The foam was created by a foam generator using a blend of liquid foaming agent and water, with a foaming agent/water ratio of 1/40.

Superplasticizer (SP) is required for the production of PULC specimens to control and maintain the workability of the fresh PULC mixtures due to the reductions caused by foam.

2.2 Mix design and proportions

The mix proportions of PULC samples are shown in Table 2. Therein, a total of four PULC mixtures were prepared with the replacement of cement proportions by slag at 0, 10, 20, and 30 %, while the contents of FA, foam, water, SP, and sand remained constants. A fixed amount of 10 % FA (by weight of total binder) was added to PULC mixtures as a binder and likewise, sand was used as aggregate by 20 wt.% of each mixture. Especially, both the water-to-binder (W/B) and aggregate-to-binder (A/B) ratios were kept at a constant value of 0.35 for all mixtures. The amount of foam was adjustable to meet the requirement of the National Standard for the target dry density of 600 kg/m^3. Besides, recent research also suggested the content of SP is approximately in the range of 0.45 to 5 % of the volume of foam agent [14] and hence, the amount of SP was adjusted to obtain a similar consistency for all mixtures. Accordingly, the proportions of SP were between 0.64 and 0.67 %.

3 Samples preparation and test methods

3.1 Mixing procedures and samples preparation

The mixing process and the sample preparation in the laboratory were described as following: Firstly, binder materials including cement, FA, and slag were mixed in a mixer until homogeneous to avert local distribution, and the time was fixed for 1 minute following ASTM C305 [15]. In fact,

Table 2 Mix proportions of PULC samples

CMs	Ingredient proportions (unit: gram)						
	Cement	FA	Slag	Foam	Water	SP	Sand
S00F00	1800	200	0	107	700	4.5	700
S10F00	1600	200	200	107	700	4.6	700
S20F00	1400	200	400	107	700	4.7	700
S30F00	1200	200	600	107	700	4.7	700

at the laboratory scale, ultra-fine materials will be shaken simultaneously to create a well-distributed mixture. At the same time, the blend of water and SP was also mixed by adding SP to water and stirring carefully. Next, slowly pour 1/3 of blended SP-water into the binder and operate the mixer within 1 minute to mix these two aforesaid compositions together. Then, sand, as well as the remaining portion of blended SP-water, was also poured into the mixer for additional 1-minute mixing. Afterward, foam obtained directly from the foam generator machine was immediately poured into the PULC mixtures and mixed for a further 2 minutes. Finally, prepared molds were filled with newly-created PULC mixtures and placed at room temperature for 24 hours before de-molding for curing in water until the days of testing.

3.2 Test methods

There were eight test methods (as summarized in Table 3) were used to evaluate the properties of PULC mixtures. First of all, mechanical properties were regarded as the most important attributes to evaluate the applicability of PULC at the hardened state and hence, in this study, compressive strength was conducted following ASTM C109 [16]. Dry density, water absorption, and drying shrinkage were then tested to analyze the overall performance of PULC samples and these mentioned experiments complied with ASTM C567 [17], C1585 [18], and C596 [19], respectively. The thermal conductivity was also measured to examine the relation between density and the voids inside PULC samples, using a portable device model, namely ISOMET 2114. Further tests such as SEM observation and XRD analysis were used to study the changes in physical and chemical structures of PULC samples and the method was described in Table 3. The application of simulation software as ANSYS APDL was accessed to model and analyze the efficiency of thermal insulation in the walls using PULC material.

The temperature distribution in the walls depends on space and time, which are determined by the basic heat transfer differential Eq. (1) [20, 21].

Table 3 Details of test programs for evaluating the performance of PULC

Test name	Test age (days)	Samples size (mm)	Reference standard
Compressive strength	3, 7, 14, 28	50 × 50 × 50	ASTM C109 [16]
Dry density	28	50 × 50 × 50	ASTM C567 [17]
Water absorption	28	50 × 50 × 50	ASTM C1585 [18]
Drying shrinkage	1, 3, 7, 14, 28	25 × 25 × 285	ASTM C596 [19]
Thermal conductivity	28	50 × 50 × 50	Using a portable device model ISOMET 2114
Numerical simulation of heat transfer through the wall	28	-	Using ANSYS APDL software
SEM observation	28	Using a broken piece from the compression test	Using scanning electron microscope of ZEISS
XRD analysis	28	Grinding broken piece from the compression test	Using XRD analyzer equipment

$$\frac{\partial}{\partial x}\left(k_x\frac{\partial T}{\partial x}\right)+\frac{\partial}{\partial y}\left(k_y\frac{\partial T}{\partial y}\right)+\frac{\partial}{\partial z}\left(k_z\frac{\partial T}{\partial z}\right)+q_v=\rho c\frac{\partial T}{\partial t}, \quad (1)$$

where: T is the temperature function depends on space and time (°C); k is the heat diffusion coefficient (m^2/s); c is the specific heat capacity of the material (kJ/kg.°C); ρ is the density (kg/m^3); q_v is the heat generated per 1 volume unit (kJ/m^3); t is the time (day).

However, the wall material is homogeneous and isotropic so $k = k_x = k_y = k_z$ and without an inner source ($q_v = 0$). Besides, the width and height of each wall are much larger than the thickness of the wall. So, we consider the problem of heat transfer as one-dimensional and steady-state heat transfer. The equation for heat transfer differential Eq. (1) can be rewritten as Eq. (2) [22]:

$$k\frac{\partial^2 T}{\partial x^2}=0\,. \quad (2)$$

The boundary conditions used in this analysis include the 1st boundary condition (temperature) and the 3rd boundary condition (convective boundary) and are described by Eq. (3):

$$T=T_{out},-\lambda\frac{\partial T}{\partial n}=h(T-T_{in})\,. \quad (3)$$

Assuming that the maximum temperature of the environment (outside the wall) is 38°C, the temperature inside the wall is 22°C and the convection coefficient of the wall surface is h = 25 W/m^2K to investigate in this study [23].

Table 4 Input data of numerical simulation

Properties of materials	PULC	Clay brick
Thermal conduction coefficient (W/m.K)	0.13	0.81
Specific heat (J/kg.K)	850	1000
Density (kg/m^3)	642	1500
Convection coefficient ($W/m^2.K$)	25	25

The data to simulate the heat transfer process for two types of walls (clay brick wall and PULC wall) are given in Table 4. In this study, the 2D element (PLANE55) of Ansys software has been used to analyze the process of heat transfer through walls [24].

4 Results and discussion

4.1 Compressive strength

The mechanical strength of PULC samples using different slag proportions is presented in Fig. 4. It can be clearly seen that the replacement of cement by slag enhanced the compressive strength of PULC samples and even, the reduction in strength with the use of 30 % slag, as compared with strength values of the 10 %- and 20 %-slag samples was still higher than the control mix without slag.

The recorded 28-day compressive strength of PULC mixes containing slag contents of 10, 20, and 30 % were 2.3, 2.5, and 2.2 MPa, respectively, while this value of slag-free mix was roughly 1.6 MPa. The highest improvement in mechanical strength of PULC mixtures was obtained at the mix incorporating 20 % slag content. In which, there was an approximately 3-fold increase in the compressive strength of PULC samples and this finding was also in good agreement with Sathish et al. [25] about the optimal proportion of slag of 20 % to achieve the maximum compressive strength of lightweight foam concrete block. Moreover, the highest development in compressive

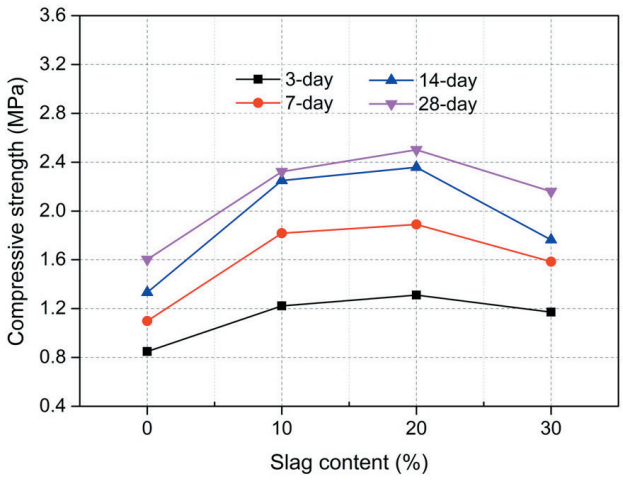

Fig. 4 Compressive strength of PULC samples

strength was also achieved at the PULC sample containing 20 % slag with an increment in compressive strength of 56 % compared with nearly 44.0 and 37.5 % increase of mixes using 10 and 30 % slag, respectively. To explain for these above-mentioned positive effects of slag on the compressive strength of PULC specimens, the chemical compositions in Table 1 revealed that slag contains a large content of Al_2O_3 (12.99 %) and CaO (38.13 %) known as strong alkaline chemicals (to be denoted as active slag particles) and sensitive to react in an alkaline environment formed from the hydration reaction between cement and water. Consequently, the interference of an appropriate amount of slag can enhance the performance of the hydration reaction. Besides, due to the ultra-fine size of slag particles, the existence of inactive slag particles may fill pores inside PULC samples, and hence, both density and compressive strength became denser and stronger. Inversely, excessive addition of slag triggered a decrease in compressive strength because the redundant of active slag is available but there is no more alkaline environment and the presence of more inactive slag particles occupied a large portion of paste, which is mainly used for aggregate.

4.2 Dry density and water absorption

According to the TCVN 9029:2017 [26], the dry density of ultra-lightweight foam concrete must be in the range of 600 ± 50 kg/m^3 as the desired dry density of 600 kg/m^3. Hence, as shown in Fig. 5, the obtained values of dry density of PULC samples met the requirement of the specification. However, the slag combination caused an inverse influence on the dry density of PULC mixtures because all mixes containing slag had slightly higher dry density than the control mix. More specifically, the dry density of PULC witnessed a gradual increase until its value reached a peak at 642 kg/m^3 with a substitution of 20 % slag, and then, it fell to 623 kg/m^3 for S30F00 mix.

Although there was a slight drop with the addition of 30 % slag (S30F00), the dry density of PULC samples using slag was still higher than the control mix of S00F00. Apparently, inactive slag particles were herein mentioned with finer particle size than cement (Fig. 2(d)) may infiltrate into air voids created by foam more easily than the coarser ones of cement. In this case, the presence of slag reduced the porosity of PULC samples. Additionally, because of the highly reactive property of slag as mentioned in Section 4.1, the use of less than 20 % slag content supplemented hydration products (mainly known as a C-S-H gel), and thereby, the air inside the void was filled by the gel during the hardening stage. This led to an increase of PULC's dry density and this result also conformed with previous research about the reduction in pore size distribution and overall porosity in foamed concrete incorporating mineral admixtures like slag [11]. On the other hand, using too much slag (exceeding 20 % in this research) accidentally reduced the dry density of PULC samples because newly created C-S-H gel by slag was occupied by the residual inactive slag particles due to most air voids were filled by an adequate amount of slag, which was smaller than 20 %. Hence, this left an unexpected void in PULC samples.

The values of water absorption of PULC mixtures are presented in Fig. 6. It can be clearly observed that the cement replacement by slag led to an improvement in the water absorption of PULC samples. However, the minimal datum was recorded at a mix containing 20 % slag after 28-day curing. The use of slag in PULC mixtures led to

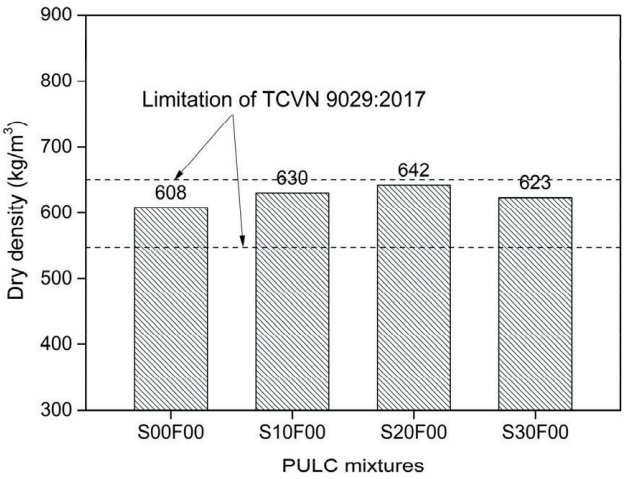

Fig. 5 Dry density of PULC samples

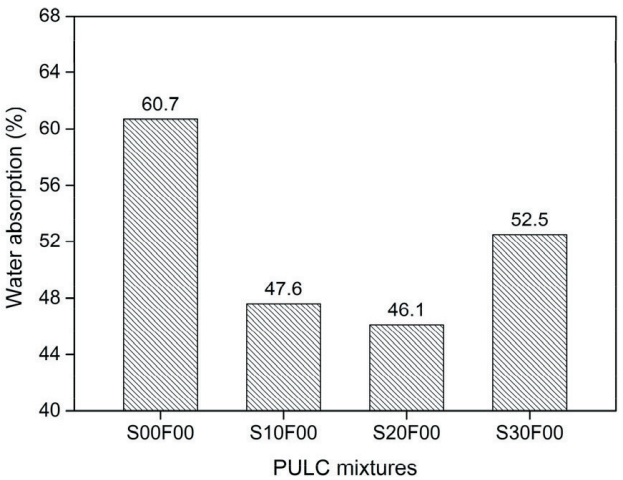

Fig. 6 Water absorption of PULC samples

the tendency of reducing water absorption from 60.7 % (control mix) to 47.6 % (10 % slag mix) and then, bottoming at 46.1 % (the substitution of 20 % slag), but this value became to growth after the threshold of 20 % replacement. The use of 10 % slag less than the water absorption approximately 22 % but an extra substitute of 10 % induced little improvement in water absorption of PULC samples (around 3.2 % reduction). Noticeably, a further substitution of slag (30 %) increased the water absorption of PULC specimens and this value was higher than the S10F00 sample (there was about 10 % difference of water absorption between two mixtures). Besides, it can be deduced that the dry density and water absorption of PULC mixtures had a correlation because the heaviest dry density of PULC samples resulted in the smallest value of water absorption, and vice versa, as shown in Figs. 5 and 6. Because of the increase of paste formed by the reaction between active slag and alkaline environment, and the intervention of ultra-inactive slag particles blocked the pores as well as capillary systems inside PULC samples.

4.3 Drying shrinkage

The effect of slag inclusion on the drying shrinkage behavior of the PULC samples is shown in Fig. 7. It is obvious that the use of slag immediately caused changes in the length of drying shrinkage samples in the early days and the differences in drying shrinkage measured at the later days were much more clear.

It could be observed from the experiment that the addition of slag reduced the volume of PULC samples and it happened severely at mix containing 20 % slag. This was also compatible with the results of density and water absorption shown in Figs. 5 and 6 because the shrinkage of PULC samples containing slag led to a reduction in water absorption and an increment in density. At one-day age, the lowest drying shrinkage was -0.0102 % of the S20F00 mix, followed by -0.0122 % of S30F00 mix, -0.0173 % of S10F00 mix, and -0.0213 % of S00F00 mix. Although there were minor differences among drying shrinkage values of samples, the trend seemed to be more closed to the density in which the reduction from S00F00 to S10F00 and bottomed at S20F00 before failing down S30F00. Furthermore, at the curing period until 28-day age, the length change of S10F00, S20F00, S30F00 samples were about 6.8 %, 24.0 %, and 15.9 % that less than the S00F00 sample, respectively. As the results of the density of PULC mixtures, the substitution of slag triggered modifications in PULC structures such as the supplement of gels. Thus, it indirectly increased drying shrinkage. At the hardening process, the more gels in cement-based materials were, the more drying shrinkage was.

4.4 Thermal conductivity

The 28-day thermal conductivity values of PULC specimens are shown in Fig. 8. Generally, the cement replacement by slag led to increases in the thermal conductivity coefficient of PULC mixtures. Particularly, the thermal conductivity values of S10F00 and S20F00 mixtures were 9.5 and 15.5 % higher than the S00F00 mixture. The PULC samples with 20 % slag obtained the highest thermal conductivity value of 0.134 W/mK. The thermal conductivity tended to reduce when slag contents exceeded 20 %. The changes in the thermal conductivity of PULC mixtures containing slag proceeded from the modification of these material structures and it was found that thermal conductivity trends are in proportional with the dry density.

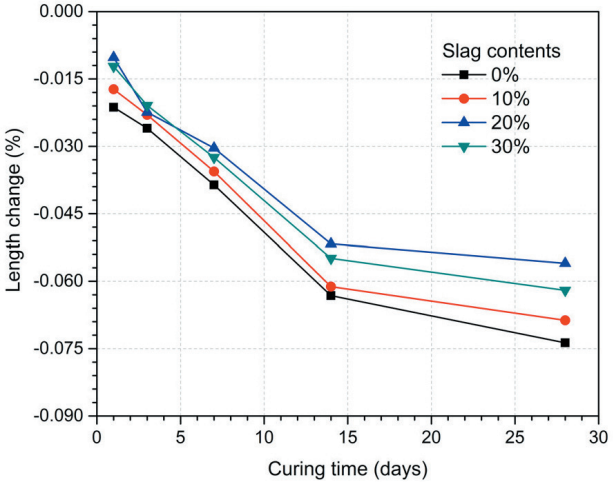

Fig. 7 Drying shrinkage of PULC samples

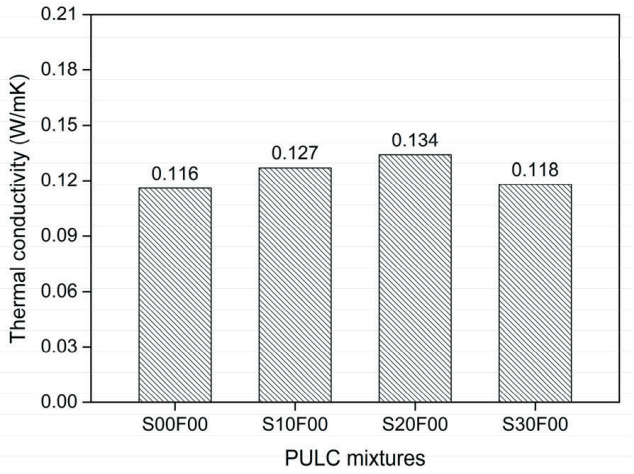

Fig. 8 Thermal conductivity of PULC samples

The increase of dry density also led to the development of thermal conductivity values of PULC samples and vice versa. The higher dry density resulted in a higher thermal conductivity material due to a more solid structure.

4.5 Numerical simulation of heat transfer through the wall

The temperature distribution in the wall simulated for two materials including PULC and clay brick is shown in Fig. 9. To compare the differences in their thermal conductivity and thermal insulation properties, the authors considered the temperature values at different spots along with the wall thickness, as Fig. 10.

It can be seen that the temperature distribution in the wall is linear (in case of not the influence of internal heat sources). The value of temperature distribution in the wall made by UPLC material was smaller than the brick in the same position. The differences in temperature between the

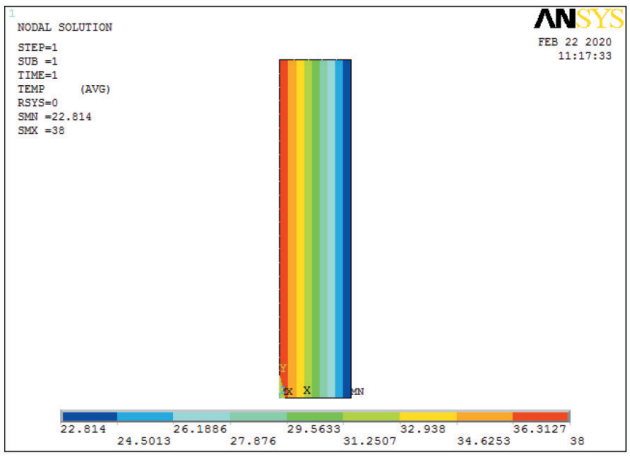

(a)

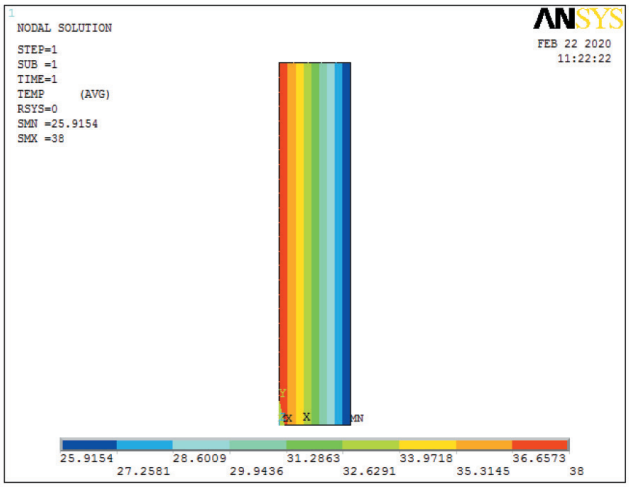

(b)

Fig. 9 The heat distribution on the wall, a) PULC wall, b) Clay brick wall

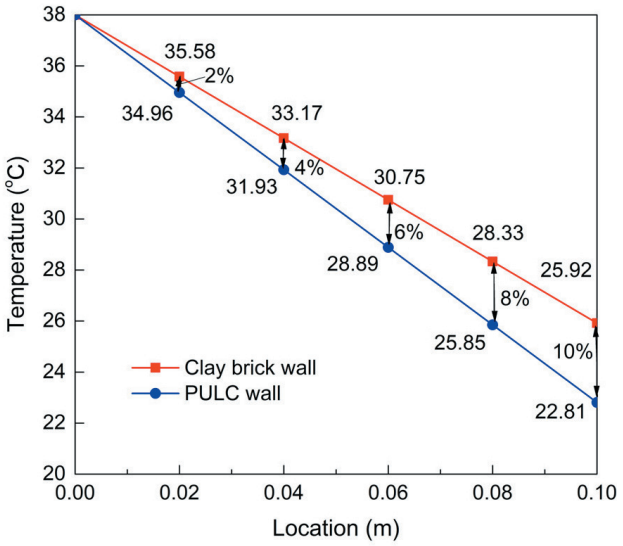

Fig. 10 The distribution of heat according to the position of the wall thickness

two types of simulated wall extended gradually in ascending order from 0 % (at the side of the wall, 0.00 m) to 10 % (at the final surveyed position, 0.1 m). The results showed that the PULC wall is quite effective in the thermal insulation in Vietnam's climate conditions.

4.6 Microstructure analysis

The interior arrangement of materials and voids inside PULC samples are revealed in microscopic images in Fig. 11. The microstructures of PULC specimens showed a well-distributed of the spheres (represented for the voids left by foam), but there were significant changes due to the use of slag. In Fig. 11(a), the size of the spheres was fairly large (the highest measured diameter d was 240 µm) and the gaps among the spheres were relatively close. The distribution of the small spheres among the bigger ones enlarged the volumes of voids inside one PULC sample and thus, lightened the density, improved thermal conductivity, but weakened the compressive strength simultaneously. Besides, the microscopic image of the S00F00 mix also presented that most of the spheres were almost unsealed because of cracks (yellow outlines) and there were porous areas (red outlines) having minor pores. Hence, that is the reason that caused the highest water absorption of the S00F00 mix. As shown in Fig. 11(b), the incorporation of a 10 % slag considerably reduced the number and the size of the spheres in PULC samples (maximum diameter was about 70 µm). Moreover, there were more rough areas with a light grey color (represented for the binder). S10F00 mix had lower water absorption and higher compressive strength than the S00F00 mix but

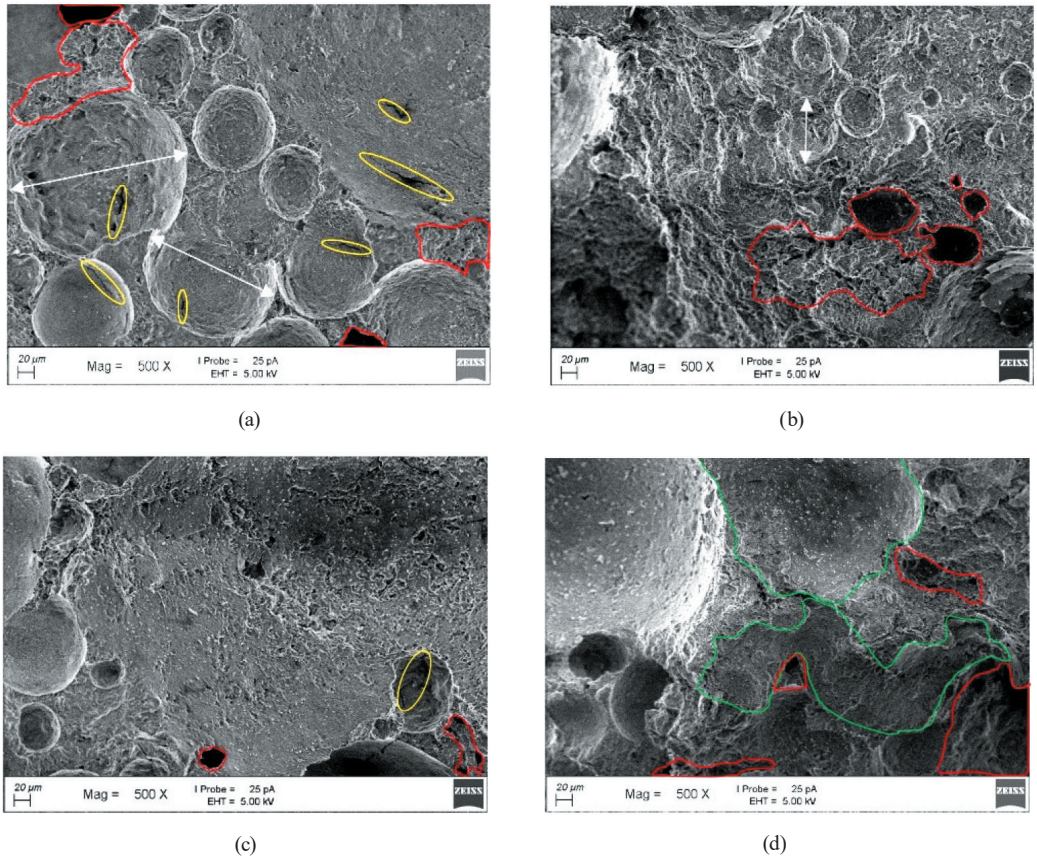

Fig. 11 SEM observation of PULC samples with various slag contents, a) S00F00, b) S10F00, c) S20F00, d) S30F00

it was superior in density, shrinkage, and thermal conductivity. It was also the same for S20F00 and S30F00 mixtures but the expressions of the microstructures slightly differed. For the S200F00 mix, the optimal amount of slag was 20 % based on previous analysis results so its microscopic images showed the best exhibition. Although there was a little porous area (as denoted in red outlines), the surface of the microstructure was highly smooth and uniform. In addition, the density of spheres was not too tight and the size of the spheres was moderate. However, the use of greater than 20 % slag distorted the S30F00 mix structure that caused a transformation in the microstructure of this sample. The microstructure surface was discrete pieces of binders (green outlines) without consistency and interspersed with porous areas. This caused changes in the mechanical and physical characteristics of the S30F00 mix such as reduction of compressive strength (due to the structure discontinuous), the increase in water absorption. However, the density, the drying shrinkage, and the thermal conductivity decreased considerably.

Fig. 12 presents the XRD patterns of PULC samples containing different amounts of slag. Obviously, the reaction among components of binder in PULC mixtures was

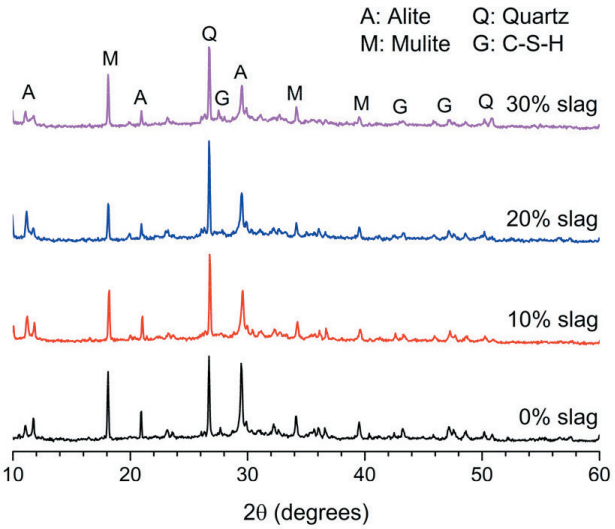

Fig. 12 XRD analysis of PULC samples with various slag contents

almost done at a high level. In Fig. 3, most of the cement phases were Alite, Belite with superior intensity, and a small amount of Pentlandite. After the reaction, there were no Pentlandite and Belite phases found in XRD patterns of all mixtures, and the intensity of Alite dropped significantly that indicated the degree of reaction between cement was high. Besides, no Belite phase found in the

XRD pattern of PULC samples after reaction indicated that the Ca^{2+} ions provided by calcium hydroxide (from the hydration process) may be consumed by silicate in slag and FA to form C-S-H (denoted as G).

Besides, there was a considerable reduction in the intensity of Mulite phase (found in the XRD pattern of FA, as shown in Fig. 3) and it was due to the involvement of SiO2 to the hydration reaction to form C-S-H gel. However, the appearance of C-S-H detected in XRD patterns of PULC samples was low intensity and this explained the reason for a low compressive strength of PULC samples. On the other hand, it can be clearly seen that the addition of FA had little effects on the chemical property of PULC mixtures because of the involvement of FA mainly based on Mulite with a small amount. There was no influence on the major component – quartz because there was no change in the intensities of the quartz phase in FA.

5 Conclusions

This study has dealt with the utilization of three proportions of slag in PULC mixtures and the performance of PULC samples in different testing conditions. It is noticeable that the substitution of cement by 20 % slag is viable to create PULC samples with the optimal performance. More specifically, salient conclusions from the analysis found in this paper can be drawn below:

1. The cement replacement by slag enhanced the compressive strength of PULC mixtures substantially and the highest value from this study was 2.5 MPa at 28-day age, which was presented for the use of 20 % slag.

2. Although having a more solid structure with the highest compressive strength, the density of the mix containing 20 % slag met the requirement for the acceptable density, and besides, the smallest amount of water absorbed was also recorded in this mix.

3. The thermal conductivity and length change of the 28-day PULC samples were in the ranges of 0.116 – 134 W/mK and (-0.0102 %) – (-0.0213%), respectively. Consequently, the addition of an appropriate proportion of slag resulted in a dense specimen and thus, increased the thermal conductivity and reduced the drying shrinkage of PULC samples. However, the outcomes from the simulation of heat transfer through the wall modeled with PULC material was still smaller than the clay brick wall, indicating the effectiveness of PULC material in terms of thermal isolation.

4. Furthermore, the SEM images of the PULC samples revealed dense microstructures of PULC samples incorporating slag, especially the PULC mix containing 20 % slag showed the smoothest and the most uniform microstructure. Thereby, the microscopic images helped to interpret the reasons for changes in engineering properties of PULC mixtures caused by the addition of slag. In addition, the XRD patterns of the PULC samples pointed out the advent of C-S-H gels when using slag, contributing to the improvement of the PULC's engineering properties.

References

[1] Li, H., Xu, W., Yang, X., Wu, J. "Preparation of Portland cement with sugar filter mud as lime-based raw material", Journal of Cleaner Production, 66, pp. 107–112, 2014. https://doi.org/10.1016/j.jclepro.2013.11.003

[2] Provis, J. L., van Deventer J. S. J. "Alkali Activated Materials", Springer, Dordrecht, Netherlands, 1986. https://doi.org/10.1007/978-94-007-7672-2

[3] Suhendro, B. "Toward Green Concrete for Better Sustainable Environment", Procedia Engineering, 95, pp. 305–320, 2014. https://doi.org/10.1016/j.proeng.2014.12.190

[4] Othuman, M. A., Wang, Y. C. "Elevated-temperature thermal properties of lightweight foamed concrete", Construction and Building Materials, 25(2), pp. 705–716, 2011. https://doi.org/10.1016/j.conbuildmat.2010.07.016

[5] Richard, T., Dobogai, J., Gerhardt, T., Young, W. "Cellular concrete - A potential load-bearing insulation for cryogenic applications?", IEEE Transactions on Magnetics, 11(2), pp. 500–503, 1975. https://doi.org/10.1109/TMAG.1975.1058746

[6] Nath, P., Sarker, P. K. "Effect of GGBFS on setting, workability and early strength properties of fly ash geopolymer concrete cured in ambient condition", Construction and Building Materials, 66, pp. 163–171, 2014. https://doi.org/10.1016/j.conbuildmat.2014.05.080

[7] Gholampour, A., Ozbakkaloglu, T. "Performance of sustainable concretes containing very high volume class-F fly ash and ground granulated blast furnace slag", Journal of Cleaner Production, 162, pp. 1407–1417, 2017. https://doi.org/10.1016/j.jclepro.2017.06.087

[8] Esmaily, H., Nuranian, H. "Non-autoclaved high strength cellular concrete from alkali activated slag", Construction and Building Materials, 26(1), pp. 200–206, 2012. https://doi.org/10.1016/j.conbuildmat.2011.06.010

[9] Yang, K.-H., Lee, K.-H., Song, J.-K., Gong, M.-H. "Properties and sustainability of alkali-activated slag foamed concrete", Journal of Cleaner Production, 68, pp. 226–233, 2014. https://doi.org/10.1016/j.jclepro.2013.12.068

[10] Gowri, R., Anand, K. B. "Utilization of fly ash and ultrafine GGBS for higher strength foam concrete", IOP Conference Series: Materials Science and Engineering, 310, Article no.: 012070, 2018. https://doi.org/10.1088/1757-899X/310/1/012070

[11] Gowripalan, N. "Effect of Curing on Durability", Concrete International, 12(2), pp. 47–54, 1990. [online] Available at: https://www.concrete.org/publications/internationalconcreteabstractsportal/m/details/id/2528

[12] Teoh, C. Y. "Performance evaluation of steel slag as natural aggregates replacement in asphaltic concrete", [pdf] Master thesis, Universiti Sains Malaysia, 2008. Available at: https://core.ac.uk/download/pdf/11933932.pdf

[13] ASTM "ASTM C618-19 Standard Specification for Coal Fly Ash and Raw or Calcined Natural Pozzolan for Use in Concrete", ASTM International, West Conshohocken, PA, USA, 2019. https://doi.org/10.1520/C0618-19

[14] Jezequel, P.-H., Mathonier, B. "Foamed concrete", Geneva, Switzerland, WO2011/101386 A1, 2014. [online] Available: https://patents.google.com/patent/WO2011101386A1/en

[15] ASTM "ASTM C305-20 Standard Practice for Mechanical Mixing of Hydraulic Cement Pastes and Mortars of Plastic Consistency", ASTM International, West Conshohocken, PA, 2020. https://doi.org/10.1520/C0305-20

[16] ASTM "ASTM C109/C109M-20b Standard test Method for Compressive Strength of Hydraulic Cement Mortars (Using 2-in. or [50-mm] Cube Specimens)", ASTM International, West Conshohocken, PA, USA, 2020. https://doi.org/10.1520/C0109_C0109M-20B

[17] ASTM "ASTM C567/C567M-19 Standard Test Method for Determining Density of Structural Lightweight Concrete", ASTM International, West Conshohocken, PA, USA, 2019. https://doi.org/10.1520/C0567_C0567M-19

[18] ASTM "ASTM C1585-20 Standard Test Method for Measurement of Rate of Absorption of Water by Hydraulic-Cement Concretes", ASTM International, West Conshohocken, PA, USA, 2020. https://doi.org/10.1520/C1585-20

[19] ASTM "ASTM C596-18 Standard Test Method for Drying Shrinkage of Mortar Containing Hydraulic Cement", ASTM International, West Conshohocken, PA, USA, 2018. https://doi.org/10.1520/C0596-18

[20] Majeed, R. H. "Effect of Temperature Difference on the Steady State Time Using ANSYS", Journal of University of Babylon for Engineering Sciences, 26(8), pp. 147–156, 2018. [online] Available at: https://iasj.net/iasj?aId=157567&func=fulltext

[21] Biondini, F., Nero, A. "Cellular Finite Beam Element for Nonlinear Analysis of Concrete Structures under Fire", Journal of Structural Engineering, 137(5), pp. 543–558, 2011. https://doi.org/10.1061/(ASCE)ST.1943-541X.0000307

[22] Huynh, T. P., Pham, V. H., Le, T. T. T., Ngo, S. H., Nguyen, T. C. "Ảnh hưởng của việc thay thế một phần xi măng bằng tro bay đến các đặc tính kỹ thuật của bê tông bọt siêu nhẹ" (Effect of partial replacement of Portland cement by fly ash on engineering characteristics of ultra-lightweight foamed concrete), Vietnam Journal of Construction, 10, pp. 67–71, 2019. (in Vietnamese)

[23] Du, H., Hu, X., Zhang, B., Yao, M. "Numerical simulation on behaviour of timber-concrete composite beams in fire", IOP Conference Series: Earth and Environmental Science, 81, Article number: 012148, 2017. https://doi.org/10.1088/1755-1315/81/1/012148

[24] Kumar, P., Kodur, V. K. R. "Modeling the behavior of load bearing concrete walls under fire exposure", Construction and Building Materials, 154, pp. 993–1003, 2017. https://doi.org/10.1016/j.conbuildmat.2017.08.010

[25] Sathish, P., Neeladharan, C., Ilakkiya, K., Jeevitha, N., Mageshwari, R., Nivetha, P. "Behaviour of Light Weight Foam Concrete Block By Using Ggbs and Foaming Agent", International Journal of Advanced Research Trends and Engineering and Technology, 5(5), pp. 109–111, 2018. [online] Available at: https://www.researchgate.net/publication/324951583_Behaviour_of_Light_Weight_Foam_Concrete_Block_by_using_GGBS_and_Foaming_Agent

[26] TCVN 9029:2017 "Bê tông nhẹ – Sản phẩm bê tông bọt và bê tông khí không chưng áp – Yêu cầu kỹ thuật" (Lightweight concrete – Foam concrete and non-autoclaved concrete products – Specification), Ministry of Science and Technology, Ha Noi, Vietnam, 2017. (in Vietnamese) [online] Available at: https://vanbanphapluat.co/tcvn-9029-2017-be-tong-nhe-san-pham-be-tong-bot-va-be-tong-khi-khong-chung-ap